

Probing the Structure of Lensing Galaxies with Quadruple Lenses: The Effect of the “External” Shear

Hans J. Witt [★]

Astrophysikalisches Institut Potsdam, An der Sternwarte 16, 14482 Potsdam, Germany

Shude Mao [†]

Max-Planck-Institute für Astrophysik, Karl-Schwarzschild-Strasse 1, 85740 Garching, Germany

Accepted Received; in original form

ABSTRACT

We study a general elliptical potential of the form $\psi(x^2 + y^2/q^2)$ ($0 < q \leq 1$) plus an additional shear (with an arbitrary direction) as models for the observed quadruple lenses. It is shown that a minimum additional shear is needed even just to reproduce the observed positions alone. We also obtain the dependence of the axial ratio, q , on the orientation of the major axis of potential. A general relation also exists between the shear, the position angle and axial ratio of the lensing galaxy. The relation shows a generic degeneracy in modelling quadruple lenses. In particular, it shows that only the ratio of the ellipticity, $\epsilon \equiv (1-q^2)/(1+q^2)$, to the magnitude of shear, γ can be determined. All these results are valid *regardless* of the radial profile of the potential. Our formalism applies when the galaxy position is observed, which is the case for seven of the eight known quadruple lenses. Application to these seven cases reveals two quadruple lenses CLASS 1608+656 and HST 12531–2914, requiring highly significant shear with magnitude ≈ 0.2 . For HST 12531–2914, there must be a misalignment between the major axis of light and the major axis of potential (mass). We conclude that detailed modelling of quadruple lenses can yield valuable quantitative information about the shape of lensing galaxies and their dark matter halos.

Key words: galaxies: structure – gravitational lensing – quasars: individual (CLASS 1608+656, HST 12531–2914)

1 INTRODUCTION

Up to now, more than twenty multiply imaged quasars have been discovered, with roughly half double and half quadruple lenses (Keeton & Kochanek 1996, hereafter KK96, see also Schneider, Ehlers & Falco 1992, Blandford & Narayan 1992 and Kochanek & Hewitt 1996 for general reviews). These systems, in particular the quadruple lenses, provide a unique tool to probe the potentials of galaxies (e.g., Kochanek 1991; Wambsganss & Paczyński 1994; Witt, Mao & Schechter 1995). Recently, Keeton, Kochanek & Seljak (1996) found that while simple models such as singular isothermal density ellipsoids provide a reasonable statistical model for the whole sample, no individual quadruple system is well fitted by such models. They found numerically that an additional shear term can drastically reduce χ^2 in fitting while changing the radial distribution of the potential helps little. As only a limited number of radial profiles (such as power laws) have been explored numerically, it is not clear whether the bad fits can still be due to our incomplete knowledge of the radial profile of galaxies. In this paper, we study a general class of elliptical potentials of the form $\psi(x^2 + y^2/q^2)$, where q denotes the axial ratio of the elliptical potential. We show that a minimum additional shear is required even if one is trying to fit only the observed positions. We also obtain analytical formulae for the axial ratio and orientations of the potential and shear. This implies some generic degeneracy in modelling of quadruple lenses. Our formalism applies *regardless* of the functional form of ψ , as long as the lensing galaxy position is observed.

The results presented here (§2) complement the study by Keeton et al. (1996) and provide an analytical understanding of their results. Our analytical formalism makes it possible to check quickly whether any elliptical potential or density distribution without shear can work at all without computing χ^2 . We apply the formalism to seven of the eight known quadruple lenses, including three of the four quadruple lenses studied by Keeton et al. (1996). Our results are consistent with theirs for these three. For two of the other four cases, HST 12531–2914 and CLASS 1608+656, we found that the minimum shear required is $\gtrsim 0.2$. For HST 12531–2914, the major axis of potential must be misaligned with that of the light. The origin of the large additional shear and its implications are discussed in the last section.

* E-mail: hwitt@aip.de

† E-mail: smao@mpa-garching.mpg.de

2 ELLIPTICAL POTENTIAL PLUS SHEAR

Both the elliptical density and potential distributions are widely used in the literature to model gravitational lenses (e.g., Blandford & Kochanek 1987, Kochanek & Blandford 1987, Kormann, Schneider, & Bartelmann 1994a,b). These two distributions resemble each other when the ellipticity is small (Kassiola & Kovner 1993), which is generally the case for the known quadruple lenses. We will use the elliptical potential model due to its analytical simplicity. Our results should apply to the elliptical density distribution almost equally well. To be quadruply lensed by an elliptical potential, the source must be located closely behind the centre of the lensing galaxy. For a pure elliptical potential, the possible locations of the images and the lensing galaxy are highly restricted (Witt 1996, hereafter W96). In reality, the image positions and flux ratios will depart from those predicted by a pure elliptical potential. For example, large scale structure and/or other galaxies along the line of sight can distort the image configuration. In addition, any departure of the galactic potential from the idealized elliptical form can produce deviations as well. As the pure elliptical potential can reproduce the overall observed image configuration quite well, a reasonable approach for further refinement is to model all the other perturbations as an additional shear term in the lens equation (Kovner 1987). This is the approach we will adopt here, as in Keeton et al. (1996).

We therefore assume the potential can be modelled as a two-dimensional elliptical potential plus an additional shear in an arbitrary direction. The elliptical potential is by definition given by $\psi(r_e)$, where $r_e \equiv x^2 + y^2/q^2$, and q ($0 < q \leq 1$) is the axial ratio of the potential. The centre of the galaxy is always located at the origin. For clarity, we first assume that the x -axis coincides with the major axis of the lensing potential. The results derived in this special coordinate system (which we term as the major axis frame) are then generalized to the case with an arbitrary major axis orientation afterwards. Throughout the paper, all the quantities measured in a general coordinate system will have a prime superscript to avoid confusion with those measured in the major axis frame.

The (projected) surface mass distribution is given by $\Delta\psi = 2\kappa(x, y)$, where $\kappa(x, y) = \Sigma(x, y)/\Sigma_{\text{crit}}$ is expressed in units of the critical surface mass density Σ_{crit} which depends on the distances to the deflector and the source (cf. Schneider et al. 1992). The two-dimensional deflection angle is then simply given by the derivatives of the potential, $\boldsymbol{\alpha} = \nabla\psi$ plus the two

terms related to the shear. The lens equation can be written as

$$\xi = x + \gamma_1 x + \gamma_2 y - \frac{\partial\psi(x^2 + y^2/q^2)}{\partial x} = x + \gamma_1 x + \gamma_2 y - \frac{\partial\psi(r_e)}{\partial r_e} 2x, \quad (1)$$

$$\eta = y + \gamma_2 x - \gamma_1 y - \frac{\partial\psi(x^2 + y^2/q^2)}{\partial y} = y + \gamma_2 x - \gamma_1 y - \frac{\partial\psi(r_e)}{\partial r_e} \frac{2y}{q^2}, \quad (2)$$

where (ξ, η) denotes the (unknown) source position and the magnitude of the shear is given by $\gamma = \sqrt{\gamma_1^2 + \gamma_2^2}$. The shear can also be written in a ‘‘vector’’ form $(\gamma_1, \gamma_2) = (\gamma \cos 2\theta_\gamma, \gamma \sin 2\theta_\gamma)$ ($0 \leq \theta_\gamma < \pi$). Notice that the factor of 2 before θ_γ arises because the shear is not really a vector but a tensor. When the shear is acting on-axis, we have $\theta_\gamma = 0, \gamma_2 = 0$. The shear is maximum off-axis when $\gamma_1 = 0$, i.e., when $\theta_\gamma = 45^\circ$, or 135° .

For quadruple lenses, the positions of the four images obey eqs. (1) and (2), therefore for each of the four images we can eliminate the factor $\partial\psi(r_e)/\partial r_e$ to obtain the following equation:

$$\frac{\xi - x_i - \gamma_1 x_i - \gamma_2 y_i}{\eta - y_i - \gamma_2 x_i + \gamma_1 y_i} = q^2 \frac{x_i}{y_i} \quad \text{for } i = 1, \dots, 4. \quad (3)$$

In the next three subsections, we will use eq. (3) as basis to derive analytical results in this paper.

2.1 Lower Limit On the Additional Shear

Using the four equations as in eq.(3), we can eliminate first q and then ξ and η , which leads us to the following equation:

$$\gamma_1 a_1 + \gamma_2 a_2 + a_3 = 0, \quad (4)$$

where the coefficients a_1, a_2 and a_3 depend on the four relative image positions, and are given by

$$a_1 = (x_1^2 + y_1^2)f_{234} - (x_2^2 + y_2^2)f_{341} + (x_3^2 + y_3^2)f_{412} - (x_4^2 + y_4^2)f_{123}, \quad (5)$$

$$a_2 = -y_1^2 h_{234} + y_2^2 h_{341} - y_3^2 h_{412} + y_4^2 h_{123}, \quad (6)$$

$$a_3 = (x_1^2 - y_1^2)f_{234} - (x_2^2 - y_2^2)f_{341} + (x_3^2 - y_3^2)f_{412} - (x_4^2 - y_4^2)f_{123}, \quad (7)$$

with the functions f_{ijk} and h_{ijk} defined as

$$f_{ijk} = x_i y_i [x_j y_k - x_k y_j] + x_j y_j [x_k y_i - x_i y_k] + x_k y_k [x_i y_j - x_j y_i] \quad (8)$$

$$h_{ijk} = x_i^2 [x_j y_k - x_k y_j] + x_j^2 [x_k y_i - x_i y_k] + x_k^2 [x_i y_j - x_j y_i]. \quad (9)$$

Note that $f_{ijk}, h_{ijk}, a_1, a_2,$ and a_3 are all odd under the permutation of any two indices.

When we derived eq. (4) we assumed that the major axis of the lensing potential is along the x -axis. In practice, it is usually more difficult to measure the orientation of the galaxy than to measure its position and those of the images. In any case, what we measure is the position angle of the light distribution, not that of the potential (mass) which enters the lens equation. Hence, we need to generalize eq. (4) to the case when the major axis of the galaxy potential is unknown, i.e., we need to investigate what happens to the coefficients a_1 , a_2 and a_3 when the major axis of the lensing galaxy is rotated by an angle θ_G ($-\pi/2 < \theta_G \leq \pi/2$). The positions of the images in the new coordinate system, (x'_i, y'_i) , are related to those measured in the major axis coordinate system, (x_i, y_i) , by

$$x_i = x'_i \cos \theta_G + y'_i \sin \theta_G, \quad (10)$$

$$y_i = -x'_i \sin \theta_G + y'_i \cos \theta_G, \quad (11)$$

for $i = 1, \dots, 4$.

In the appendix we show that a_3 is rotationally invariant, i.e.,

$$a_3 = a'_3. \quad (12)$$

Since $\theta_\gamma = \theta'_\gamma - \theta_G$, the shear tensor transforms like

$$\gamma_1 = \gamma \cos(2\theta_\gamma) = \gamma'_1 \cos(2\theta_G) + \gamma'_2 \sin(2\theta_G), \quad (13)$$

$$\gamma_2 = \gamma \sin(2\theta_\gamma) = -\gamma'_1 \sin(2\theta_G) + \gamma'_2 \cos(2\theta_G). \quad (14)$$

To satisfy the invariance of a_3 , (a_1, a_2) must transform like a tensor as well. It is easy to verify that (a_1, a_2) transforms as follows

$$a_1 = a'_1 \cos(2\theta_G) + a'_2 \sin(2\theta_G), \quad (15)$$

$$a_2 = -a'_1 \sin(2\theta_G) + a'_2 \cos(2\theta_G). \quad (16)$$

Substituting eqs. (12), (15), and (16) into eq. (4), one obtains

$$\gamma'_1 a'_1 + \gamma'_2 a'_2 + a'_3 = 0. \quad (17)$$

The equation has the same form as eq. (4), but now all the quantities are evaluated in the general coordinate system. Replacing the two shear components by $\gamma'_1 = \gamma \cos(2\theta'_\gamma)$ and $\gamma_2 = \gamma \sin(2\theta'_\gamma)$ yields

$$\gamma [a'_1 \cos(2\theta'_\gamma) + a'_2 \sin(2\theta'_\gamma)] + a'_3 = 0. \quad (18)$$

The above equation can be rewritten as

$$\gamma \sqrt{a'^2_1 + a'^2_2} \sin(2\theta'_\gamma + \varphi') + a'_3 = 0, \quad (19)$$

where φ' ($-\pi < \varphi' \leq \pi$) is the polar angle of the vector (a'_2, a'_1) . Eq. (19) implies that, to fit the observed positions, a minimum shear is required:

$$\gamma_{\min} = \frac{|a'_3|}{\sqrt{a_1'^2 + a_2'^2}} = \frac{|a_3|}{\sqrt{a_1^2 + a_2^2}}, \quad \text{when} \quad \theta'_\gamma = \theta'_{\gamma, \min} \equiv -\frac{\varphi'}{2} - \frac{\pi}{4} \text{sign}(a'_3) + k\pi, \quad (20)$$

where throughout the paper k is an integer that make the angle at the left hand side of the equation (θ'_γ here) fall into the right range.

We now make some general remarks about eq. (20). First, the minimum shear is required no matter what the radial profile is as long as the iso-potential contours are ellipses. This easily explains why changing radial profiles, such as adding a core radius or changing the slope of a power law radial profile, will not improve the fitting much (Kochanek 1991; Wambsganss & Paczyński 1994; Keeton et al. 1996). Second, as the coefficients a_1, a_2 and a_3 involve differences of permuting terms, the required (minimum) shear is likely to be very sensitive to the accuracy of positions. High quality relative astrometry of galaxy and image positions are thus much desirable.

2.2 Axial Ratio of Lensing Galaxy

In this subsection we discuss whether the axial ratio q can be restricted. To do this, we again start with eq.(3) and eliminate successively ξ, η using three image coordinates $i = 1, 2, 3$, after which we obtain

$$(1 + \gamma_1 - q^2(1 - \gamma_1))f_{123} = \gamma_2[q^2h_{123} - y_1^2(x_2y_3 - x_3y_2) - y_2^2(x_3y_1 - x_1y_3) - y_3^2(x_1y_2 - x_2y_1)]. \quad (21)$$

where f_{132} and h_{132} are defined as in eqs. (8) and (9). If $\gamma_2 \neq 0$, then we can use the fourth image position to eliminate γ_1 or γ_2 . By eliminating one shear component the other shear component factorizes out of the equation simultaneously. Therefore we obtain an equation which depends only on the relative image positions and the axial ratio:

$$q^2 = \frac{y_1^2 f_{234} - y_2^2 f_{341} + y_3^2 f_{412} - y_4^2 f_{123}}{x_1^2 f_{234} - x_2^2 f_{341} + x_3^2 f_{412} - x_4^2 f_{123}} = \frac{a_1 - a_3}{a_1 + a_3}, \quad (22)$$

where a_1 and a_3 are given by eqs. (5) and (7). We can easily generalize eq. (22) to an arbitrary major axis orientation by using eqs. (15) and (12):

$$q^2 = \frac{a'_1 \cos(2\theta_G) + a'_2 \sin(2\theta_G) - a'_3}{a'_1 \cos(2\theta_G) + a'_2 \sin(2\theta_G) + a'_3} = \frac{\sin(\varphi' + 2\theta_G) - \text{sign}(a'_3)\gamma_{\min}}{\sin(\varphi' + 2\theta_G) + \text{sign}(a'_3)\gamma_{\min}}, \quad (23)$$

with φ' as defined below eq. (19). Since q^2 must be positive, eq. (23) provides a general (but weak) constraint on the axis orientation (cf. Fig. 3). Clearly q achieves a maximum,

$$q_{\max} = \left(\frac{1 - \gamma_{\min}}{1 + \gamma_{\min}} \right)^{1/2}, \quad \text{when} \quad \theta_G = \theta_{G, \max} \equiv -\frac{\varphi'}{2} + \frac{\pi}{4} \text{sign}(a'_3) + k\pi. \quad (24)$$

As shown in W96, it is impossible to determine q for a pure elliptical potential with a shear acting along the axis, i.e., when $\gamma_2 = 0$; it therefore seems rather peculiar that for the more general shear case it is actually possible to do so. The reason for this peculiarity is rooted in the properties of an pure elliptical potential. Due to its highly symmetric and self-similar shape of the iso-potential contours, the positions of the images and galaxy are highly restricted. For example, the location of the lensing galaxy is restricted to a hyperbola-like curve and the image positions in such a potential must fulfil the identities $f_{123} = f_{134} = f_{234} = f_{124} = 0$ (W96). This can be seen from eq. (21) by setting $\gamma_2 = 0$. Then we must have $[1 + \gamma_1 - q^2(1 - \gamma_1)]f_{132} = 0$, which requires either $q^2 = (1 + \gamma_1)/(1 - \gamma_1)$, $\gamma_1 < 0$ or $f_{132} = 0$. If the former condition is satisfied, using eqs. (1) and (2), it is easy to show that all the images must lie on a straight line. This image configuration clearly does not resemble the observed quadruple lenses. Therefore we must have $f_{123} = 0$. As a result q can no longer be determined. Physically we can understand it as follows: A off-axis shear on top of the elliptical potential breaks down the high symmetry required for the image positions (f_{ijk} 's are no longer required to be zero), which in turn allows us to determine the axial ratio.

As we have shown, when the shear is acting on-axis, eq. (23) cannot be applied. Numerically this implies that when the shear component (γ_2) is small, eq. (23) is likely to be unstable due to the errors in the image and galaxy positions. Therefore before applying eq. (23) it is necessary to check first whether the observed system requires an off-axis shear, using the test introduced by W96 (see §2.4). If a significant off-axis shear is indicated, the (minimum) magnitude of the additional shear can be estimated using eq. (20). If the required shear is large, then eq. (23) can be applied to restrict the axial ratio and the orientation of the major axis of potential (see below).

2.3 Orientations of Lensing Galaxy and Shear

Combining eqs. (19) and (23), we arrive at a new relation:

$$\tan(2\theta_G + \varphi') = -\frac{\sin 2\theta_\gamma}{\cos 2\theta_\gamma + \epsilon/\gamma}, \quad \epsilon \equiv \frac{1 - q^2}{1 + q^2}, \quad (25)$$

where ϵ as defined is the ellipticity of the iso-potential contours. This equation bears some similarity to eq. (22) found by Keeton et al. (1996).

Eq. (25) shows two important points. First, since only the ratio ϵ and γ enters eq. (25), there is a degeneracy between these two parameters. This can be understood as follows: an increase in ellipticity ($0 \leq \epsilon < 1$) (a decrease of axial ratio of q) stretches the images more

along the x axis, while an increase in the shear stretches the images more along the y axis, the balance between these two competing effects introduces the degeneracy. Eq. (25) also shows that even if the ellipticity and the galaxy orientation are known (e.g., if we use those for the light distribution), the shear tensor still cannot be determined uniquely (see Figs. 8 and 9 in Keeton et al. 1996).

If the potential is purely elliptical, i.e., $\theta_\gamma = 0$ ($\gamma_2 = 0$), then from eq. (25), we have

$$\theta_{G,\text{pure}} = -\frac{\varphi'}{2} \quad \text{for } \gamma_2 = 0. \quad (26)$$

The above expression can be shown to be identical to eq. (7) in W96 in this case. However, if an off-axis shear is present ($0 < \gamma_2 \lesssim 0.3$), eq. (26) is only approximately true. Combined with eq. (24), we obtain

$$|\theta_{G,\text{max}} - \theta_{G,\text{pure}}| \approx \frac{\pi}{4}. \quad (27)$$

Notice that in general, the difference between the true orientation and that obtained by using a pure elliptical potential depend on not only the direction of shear but also the ratio of ellipticity and shear as well.

2.4 Application To Known Quadruple Lenses

Eight quadruple lenses are known (see KK96 for a thorough summary). Seven of these eight systems (except H1413+117) have known galaxy and image positions; our results can be applied to study these systems. When multiple sets of positions are available, we generally took the data with the best astrometry. Detailed references are listed in the last column in Table 1. For each system, we use eq. (20) to derive the minimum shear; the results are shown in Table 1. As one can see, the required minimum shears vary significantly from system to system. For example, for 2237+0305 it is consistent with zero, while for the lens CLASS 1608+656 it is as large as 0.25. How sensitive are these estimates to the positional errors? To address this question, we used Monte Carlo simulations to generate synthetic lensed systems by assuming all the positions are uncorrelated and their errors are Gaussian. For each lens, 10,000 Monte Carlo realizations are generated, and the minimum shear is calculated for each of these. The average and standard deviation are then computed and shown in Table 1. In some cases, the distributions of the inferred minimum shear are highly non-Gaussian, especially in the case of B1422+231. It has an almost flat distribution of minimum shear between 0 to ≈ 0.3 . For MG 0414+0534 the minimum shear is about 0.1 (2σ significant). However, it remains

Table 1. Minimum Shear Required For Known Quadruple Lenses

Object	γ_{\min}	σ_{image}	σ_{galaxy}	Reference
2237+0305	0.0092 (0.0099 \pm 0.0063)	0.005	0.005	C91
PG 1115+080	0.053 (0.058 \pm 0.034)	0.005	0.05	K93
MG 0414+0534	0.12 (0.12 \pm 0.058)	0.0003	0.05	KMH96; F96
CLASS 1608+656	0.25 (0.25 \pm 0.027)	0.01	0.01	M95; S95
B 1422+231	0.11 (0.165 \pm 0.125)	0.002	0.05	P92; YE94
HST 14176+5226	0.037 (0.040 \pm 0.027)	0.03	0.03	R95; R96
HST 12531–2914	0.18 (0.18 \pm 0.058)	0.03	0.03	R95; R96

Note.— γ_{\min} is the minimum shear which is required to fit the positions of the observed image and lensing galaxy. The mean and standard deviation (listed in brackets) for each system in γ_{\min} are derived from 10,000 Monte Carlo simulations for the positions assuming the positional errors are Gaussian and uncorrelated. σ_{image} and σ_{galaxy} denotes the astrometric accuracy (in arcseconds) of the image positions and the lensing galaxy (cf. KK96). One known quadruple lens H1413+117 is not listed here because no galaxy position is yet available, therefore our formalism does not apply.

unclear whether the shear is due to the less accurate galaxy position [‡]. Two cases, CLASS 1608+656 (Meyers et al. 1995, hereafter M95) and HST 12531–2914 (Ratnatunga et al. 1995, 1996, hereafter R95, R96) require even more significant shears than MG 0414+0534. We will therefore concentrate on these two systems below.

The image configurations of these two systems, HST 12531–2914 and CLASS 1608+656 are shown in Figs. 1 and 2, respectively. For a pure elliptical potential, the lensing galaxy position must lie on the hyperbolic-like curves in these figures. Both systems show a significant deviation these curves, suggesting the presence of a significant off-axis shear (cf. W96). This is consistent with the highly significant minimum shear derived above (cf. Table 1).

As HST 12531–2914 and CLASS 1608+656 clearly need some large off-axis additional shear, eq. (23) can therefore be applied to both systems. In Fig. 3, we plot the dependence of the axial ratio q on the position angle θ_P for these two systems. Note the position angle is conventionally measured from north (positive y axis) through east (minus x axis). If we limit the range of θ_P to be from 0 to π , then it is related to θ_G by

$$\theta_P = \theta_G + \pi/2. \quad (28)$$

If we (artificially) fit a pure elliptical potential model to both systems, we obtain position angles $\theta_P = 18.6^\circ$, $\theta_P = 68.5^\circ$ for HST 12531–2914 and CLASS 1608+656, respectively (cf.

[‡] The Ellithorpe (1995) image position (see KK96) would imply a considerable minimum shear (≈ 0.16) for MG 0414+0534. However, his relative position of image C is not compatible with the recent observations of Falco et al. (1996) and Katz et al. (1996).

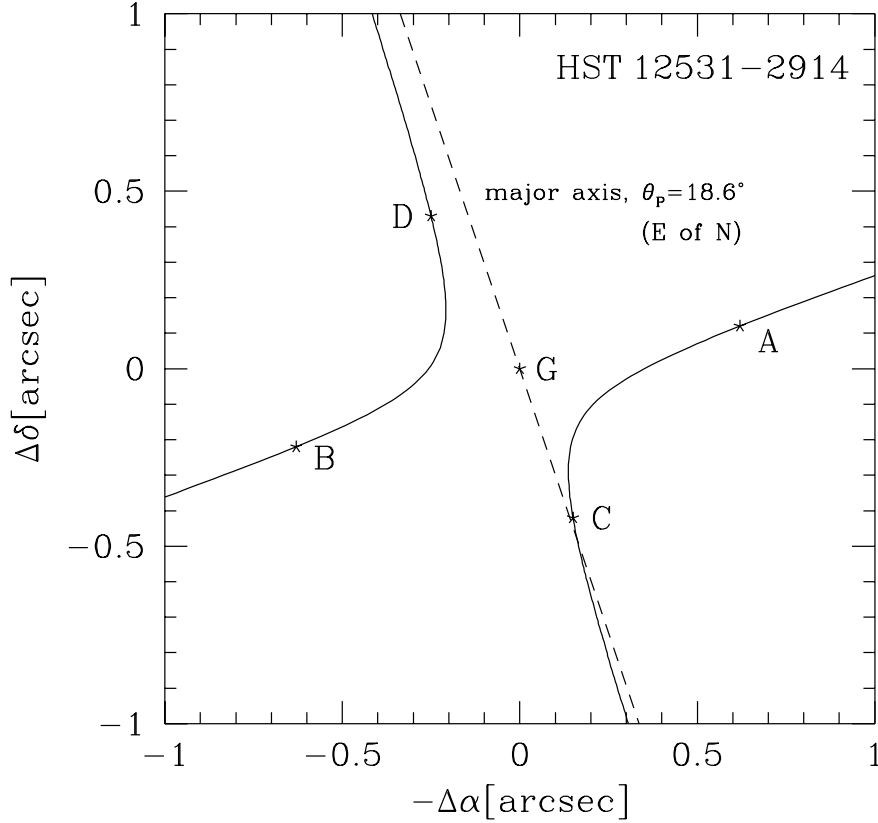


Figure 1. Image configuration of HST 12531–2914. North is up and east is to the left. The errorbar in the galaxy position is about 0.03 arcsecond (cf. Table 1). The solid line indicates the possible location of the lensing galaxy when we assume a pure elliptical potential. For this model, the galaxy and image positions lie on the same curves. The offset of the galaxy position from the predicted curves indicates the presence of a large shear. The expected position angle, θ_P , measured from north through east, for a pure elliptical potential is indicated with a dashed line (cf. W96). The observed position angle for the light distribution is $22^\circ.6 \pm 0.5$ from the HST image in the F606W filter (R95; R96).

Fig. 3). For HST 12531–2914, this estimate is in rough agreement with the position angle of the light, $\theta_P = 22^\circ.6 \pm 0.5$ (R95). (For CLASS 1608+656, the orientation of the galaxy is unavailable.) There are a few interesting things that can be seen from Fig. 3. First for HST 12531–2914, the positional angle of light (solid line) falls in the unphysical region where q^2 is negative. This means that there must be a misalignment between the major axis of the potential and that of the light. This conclusion is valid regardless of the radial profile of the potential. From Fig. 3, if the axial ratio of the potential is identical to that of light (0.73), then $\theta_P \approx 39.5^\circ$, implying a misalignment of about 17° . Second, the q vs. θ_G curves are fairly

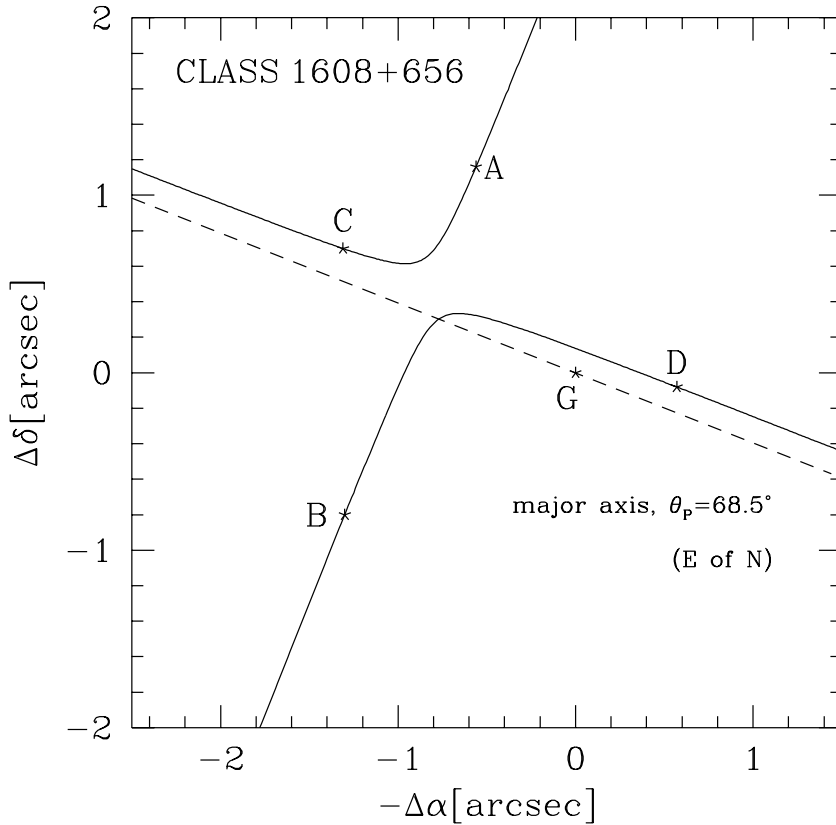


Figure 2. Image configuration of CLASS 1608+656. North is up and east is to the left. The errorbar in the galaxy position is about 0.01 arcsecond (cf. Table 1). The solid line indicates the possible location of the galaxy when we assume a pure elliptical potential. For this model, the galaxy and image positions lie on the same curves. The offset of the galaxy position from the predicted curves indicates the presence of a large shear. The expected position angle, θ_p , for a pure elliptical potential is indicated as a dashed line (cf. W96). The inferred position angle from modelling is 67° (E of N) (M95).

flat around the peak regions. This can be seen by expanding eq. (24) in Taylor series around $\theta_{G,\max}$, which leads to

$$q^2 = q_{\max}^2 - \frac{4\gamma_{\min}}{(1 + \gamma_{\min})^2} \delta\theta_G^2, \quad \theta_G = \theta_{G,\max} + \delta\theta_G. \quad (29)$$

This means that q^2 varies quadratically at the peak region. Third, although we showed that HST 12531–2914 and CLASS 1608+656 cannot be exactly fitted by a pure elliptical potential, nevertheless the models published so far did use the pure elliptical density distributions (R95, R96; M95). In these modelling, one finds the best fit parameters by minimizing a χ^2 measure. Obviously the resulting χ^2 per degree of freedom will be very large (see χ^2 in Keeton et al. 1996 for other systems). As one typically searches for the best fit axial ratio starting from an

initial guess of one, as shown in Fig. 3 the q vs. θ_G curve is nearly flat around the maximum (implying a large phase space in the multiple dimensional parameter space), we therefore expect the resulting axial ratio to be close to the maximum axial ratio. Indeed, the axial ratios for the density distribution, q_ρ , are found to be 0.37 for HST 12531–2914 (R95; R96) and 0.28 for CLASS 1608+656 (M95). Since $q \approx 2/3 + q_\rho/3$ (Binney & Tremaine 1987), we have $q = 0.83$ and 0.79 . These are very close to the maximum axial ratios from Fig. 3, $q_{\max} = 0.83$ for HST 12531–2914 and $q_{\max} = 0.78$ for CLASS 1608+656, achieved at $\theta_P = 65.3^\circ$ and 114.2° , respectively. Fourth, the position angle at the maximum axial ratio is approximately 45° away from the orientation inferred by modelling the lens galaxy as a pure elliptical potential for both systems, just as given by eq. (27).

3 DISCUSSION

We have studied a general class of models with an elliptical potential plus an additional shear. It was shown that to fit the image and galaxy positions in quadruple lenses, the additional shear has to exceed some minimum value. In addition, an analytical expression for the axial ratio is derived. We also showed that there is a complex relation between the orientations of the shear and potential, the ellipticity and the magnitude of shear. As only the ratio of the ellipticity and the magnitude of shear enters the relation, these two parameters are linearly degenerate. We emphasize our results are valid no matter what the radial profile is for the elliptical potentials. Applying the analytical results to seven of the eight known quadruple lenses, we found that two (MG 0414+0534, B 1422+231) are consistent with the presence of additional shears of the order of 0.1, while HST 12531–2914 and CLASS 1608+656 require highly significant shears of $\gtrsim 0.2$. For HST 12531–2914, we conclude that the major axes of potential and light must be misaligned, regardless of the detailed potential shape. We caution that both systems are somewhat “special”: HST 12531–2914 has very small separations between the images. The images seem to be not perfectly aligned with axes of the lensing galaxy (cf. the frames in R96). In contrast the lensed source in CLASS 1608+656 is a radio galaxy and not a quasar. It is conceivable that the small separations or the extended source size make the position measurements more difficult and the errors on their positions are under-estimated. We therefore artificially enlarged their errors by a factor of 2, and recomputed their statistical significance. CLASS 1608+656 remains 5σ significant while the significance for HST 12531–2914 has dropped to 1.7σ . The exceptional nature of

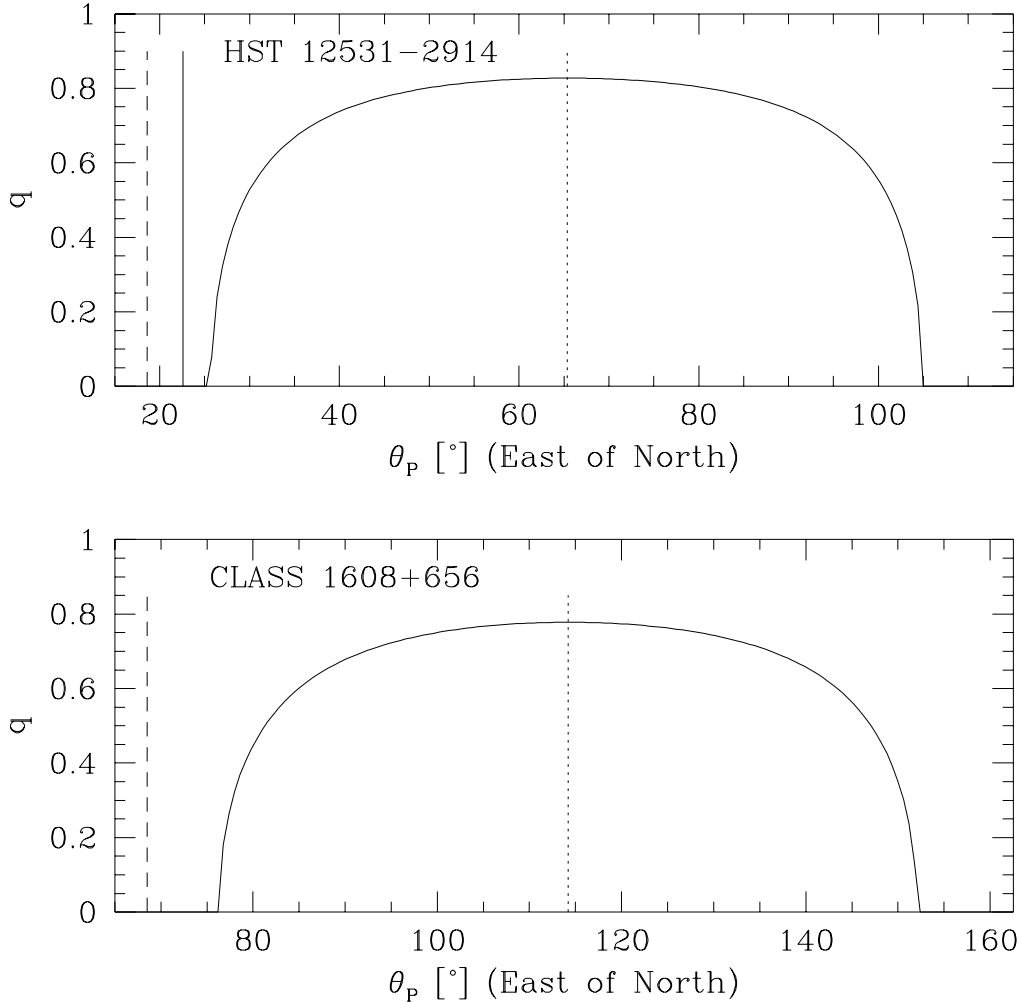


Figure 3. Dependence of the axial ratio q on the position angle θ_P for CLASS 1608+656 (bottom panels) and HST 12531-2914 (top panels). The position angle of the light distribution for HST 12531-2914 in the F606W filter is shown with the solid line. The dashed line shows the position angle of the major axis estimated by enforcing a pure elliptical potential while the dotted line shows the position angle for the maximum q (see eq. [24]). $q_{\max} = 0.78$ for CLASS 1608+656 and $q_{\max} = 0.83$ for HST 12531-2914.

CLASS 1608+656 can also be seen from the ratio of the distances between the images C and D to A and B, $\Delta\theta_{CD}/\Delta\theta_{AB} \approx 1.0$ (for HST 12531-2914 $\Delta\theta_{CD}/\Delta\theta_{AB} \approx 0.73$). For a pure elliptical isothermal sphere, we would expect $\Delta\theta_{CD}/\Delta\theta_{AB} \approx q$. CLASS 1608+656 therefore signals a substantial deviation even from the maximum possible value ($q = 0.78$), again indicating the presence of an additional shear on top of an elliptical potential.

We emphasize here that in Table 1 only the lower bound of the additional shear was derived. Computations with some test potentials indicates that $\gamma_{\min} \approx \gamma_2$ and $q_{\max} \approx q$ when $\gamma_1 \approx 0$, i.e., when $\theta_\gamma \approx 45^\circ$, or 135° . In these cases the additional shears derived are

highly significant. However, if $\gamma_1 \gtrsim \gamma_2$ the minimum shear derived using eq. (20) is usually smaller than the actual shear γ and not statistically significant. Since for CLASS 1608+656 and HST 12531–2914, the additional shears are highly significant, their directions of shear are likely to be close to 45° and the shear is close to the minimum values derived here. For B 1422+231 and PG 1115+080, Keeton et al. (1996) gives the additional shears of 0.20 and 0.09, roughly a factor of 2 larger than the predicted minimum shears, suggesting there is a significant part of shear acting along the axes. The real shears in other systems can also be easily a factor 2 or 3 larger than the predicted values.

These additional shears required are large compared with the external shears produced by large scale structure (Bar-Kana 1996, Schneider 1997), or galaxies and clusters along the line of sight (Keeton et al. 1996), which are usually of the order of a few percent. This suggests that the origin of the shear is not “external”, but introduced by the lensing galaxy internally (Keeton et al. 1996). If the shear is truly intrinsic, it will be interesting to see whether there is correlation of the additional shear with physical parameters of the lenses. For example, the potential of galaxies will be less relaxed and more irregular in a hierarchical formation scenario as the redshift increases. Therefore when a sufficient number of lenses are known, one should find some correlation between the required additional shear and the redshift of the lensing galaxy.

It is worthwhile to reflect why we need such large additional shears to model some of these observed systems. For the elliptical potential studied here (and similarly for the elliptical density distribution), the direction of the deflection angle is independent of the radial coordinates (cf. eqs. [1] and [2]). This strongly restricts the allowed image and galaxy positions (W96). Violation of these restrictions directly translates to an additional off-axis shear required in the model. The large values of the inferred additional shears illustrates that our modelling of the lens potential is too simplistic. The misalignment of the mass and luminous part of the lensing galaxy in HST 12531–2914 shows an example of possible complexities. Other possibilities such as the triaxiality of the dark halo clearly exist (see Keeton et al. 1996). All these complications make the isopotential contours more complex and possibly twisted. With the added complexities, one can presumably fit the observed positions and flux ratios better as more degrees of freedom become available. Such complexities may prove to be a nuisance in lens applications such as determining the Hubble constant. On the other hand, this means detailed modelling of quadruple lenses may also yield information about the shapes of lensing potentials and dark halos. For example, the newly discovered

quintuple lens 0024+1654 (cf. Colley, Tyson & Turner 1996) would be an excellent example to apply our formalism as the fifth image provides additional constraints. This exceptional case shows a lensed high-redshift galaxy with large image separations. Since the source is also extended, the system contains much more information that can be used to probe the potential of the lensing cluster. With more and more quadruple (or quintuple) systems discovered, we are optimistic that gravitational lenses will become an increasingly discriminating tool to study the (dark) matter distribution in galaxies.

This work was supported by a postdoctoral grant of the Deutsche Forschungsgemeinschaft (DFG) under Gz. Mu 1020/3-2 (HJW) and by the ‘‘Sonderforschungsbereich 375-95 f ur Astro-Teilchenphysik’’ der Deutschen Forschungsgemeinschaft (SM). We are very grateful to Peter Schneider for his constructive comments on the paper.

APPENDIX A: ROTATIONAL INVARIANCE OF A_3

In this appendix, we show that a_3 as defined in eq. (7) is rotationally invariant. It is easy to verify that a_3 can be written as the determinant of a 4x4 matrix:

$$a_3 = \det \begin{pmatrix} x_1^2 - y_1^2 & x_2^2 - y_2^2 & x_3^2 - y_3^2 & x_4^2 - y_4^2 \\ x_1 y_1 & x_2 y_2 & x_3 y_3 & x_4 y_4 \\ x_1 & x_2 & x_3 & x_4 \\ y_1 & y_2 & y_3 & y_4 \end{pmatrix}. \quad (\text{A1})$$

From linear algebra, this determinant can be expressed as

$$a_3 = \sum_{i,j,k,l} \epsilon(i,j,k,l) \det \begin{pmatrix} x_i^2 - y_i^2 & x_j^2 - y_j^2 \\ x_i y_i & x_j y_j \end{pmatrix} \times \det \begin{pmatrix} x_k & x_l \\ y_k & y_l \end{pmatrix}, \quad (\text{A2})$$

where (i,j,k,l) ’s are permutations of the four indices (1,2,3,4) satisfying $i < j$ and $k < l$, and $\epsilon(i,j,k,l)$ ’s are either +1 or -1 but are of no importance here, since we will show each term in the sum is rotationally invariant. To prove this, let us express the image positions in the polar coordinates, i.e., $(x_i, y_i) = (r_i \cos \theta_i, r_i \sin \theta_i)$. The determinants of the two 2x2 submatrices are then

$$\det \begin{pmatrix} x_i^2 - y_i^2 & x_j^2 - y_j^2 \\ x_i y_i & x_j y_j \end{pmatrix} = \frac{1}{2} r_i^2 r_j^2 \sin 2(\theta_j - \theta_i), \quad \det \begin{pmatrix} x_k & x_l \\ y_k & y_l \end{pmatrix} = r_k r_l \sin(\theta_l - \theta_k). \quad (\text{A3})$$

Both terms are obviously invariant under rotation. It follows that a_3 is rotationally invariant as well.

REFERENCES

- Bar-Kana, R. 1996, ApJ, 468, 17
- Blandford, R.D. & Kochanek, C. S. 1987, ApJ, 321, 658
- Blandford, R.D. & Narayan, R. 1992, ARA&A, 30, 311
- Binney, J., & Tremaine, S. 1987, Galactic Dynamics (Princeton: Princeton University Press), p60
- Crane, P. et al. 1991, ApJ, 369, L59 (C91)
- Colley, W.N., Tyson, J.A. & Turner, E.L. 1996, ApJ, 461, L83
- Ellithorpe, J.D., 1995, Ph.D. thesis, MIT
- Falco, E.E., Lehár, J., Shapiro, I.I., & Kristian, J. 1996, ApJ, submitted (F96)
- Katz, C. A., Moore, C. B., & Hewitt, J. N. 1996, preprint (astro-ph/9609104) (KMH96)
- Kassiola, A. & Kovner, I. 1993, ApJ, 417, 450
- Keeton II, C.R., Kochanek, C. S., & Seljak, U. 1996, preprint (astro-ph/9610163)
- Keeton II, C.R. & Kochanek, C.S. 1996, in Kochanek, C.S. & Hewitt, J.N. (eds.), IAU 173, Melbourne, *Astrophys. Applications of Gravitational Lensing*, Kluwer, p. 419 (KK96)
- Kochanek, C.S. 1991, ApJ, 373, 354
- Kochanek, C. S. & Blandford, R. D. 1987, ApJ, 321, 676
- Kochanek, C.S. & Hewitt, J.N. (eds.), IAU 173, Melbourne, *Astrophys. Applications of Gravitational Lensing*, Kluwer, p. 419
- Kormann, R., Schneider, P., & Bartelmann, M.: 1994a, A&A, 284, 285
- Kormann, R., Schneider, P., & Bartelmann, M.: 1994b, A&A, 286, 357
- Kovner, I. 1987, ApJ, 316, 52
- Kristian, J. et al. 1993, AJ, 106, 1330 (K93)
- Myers, S.T. et al. 1995, ApJ, 447, L5 (M95)
- Patnaik, A.R. et al. 1992, MNRAS, 259, 1P (P92)
- Ratnatunga, K.U., et al. 1995, ApJ, 453, L5 (R95)
- Ratnatunga, K.U., et al. 1996, in Kochanek, C.S. & Hewitt, J.N. (eds.), IAU 173, Melbourne, *Astrophys. Applications of Gravitational Lensing*, Kluwer, p. 323 (R96)
- Schechter, P.L. 1995, private communication in KK96 (S95)
- Schneider, P. 1997, in preparation
- Schneider, P., Ehlers, J., & Falco, E. E. 1992, *Gravitational Lenses* (Springer-Verlag: New York)
- Wambsganss, J. & Paczyński, B. 1994, AJ, 108, 1156
- Witt, H.J. 1996, ApJ, 472, L1 (W96)
- Witt, H.J., Mao, S., & Schechter, P.L. 1995, ApJ, 443, 18
- Yee, H.K.C., & Ellingson, E. 1994, AJ, 107, 28 (YE94)

This paper has been produced using the Royal Astronomical Society/Blackwell Science L^AT_EX style file.